International Scientific Colloquium
Modelling for Electromagnetic Processing
Hannover, October 27-29, 2008

Heat Exchange and Operating Gas Flow Influence on Radiation Resistant Pressure Sensor Properties

V. Geza, A. Jakovics, K. Thomsen

Abstract

A novel pressure sensor is investigated numerically. Operation of this sensor is determined by mechanical stresses and heat exchange. Estimation of deformations and heat transfer was done using programs ANSYS and ANSYS CFX. Numerical model was calibrated to fit experimental results. Conclusions about significance of heat exchange, thermal stresses and overall action of sensor were made.

1. General information

A novel concept for measuring pressures in conditions which requires resistance against radiation is developed in PSI, but it still needs further investigation and numerical simulation. It is important to find parameters for sensor to ensure pressure measurements with certain precision in 1-10 bar parameter range. Main task of this work is to model pressure sensor using commercial mathematical modelling programs ANSYS and ANSYS CFX, optimize model parameters to fit experimental data and to evaluate role of different physical effects, especially role of heat and mass transfer.

2. Modeled equipment

The equipment consists of two symmetric loud speaker shaped membranes which are welded together in the outer part W. Figure 1 shows 2D axisymmetric model geometry. Approximate diameter of whole system is 77 mm. It is possible to pump gas in cavities CT and CB. There is vacuum in cavity V. When no gas is pumped, the two membranes MT and MB just touch in a contact surface C, no large contact pressure occurs. Heating at point HT causes a local rise in temperature. With its supporting membrane MT made of material with low thermal conductivity a significant temperature gradient to the

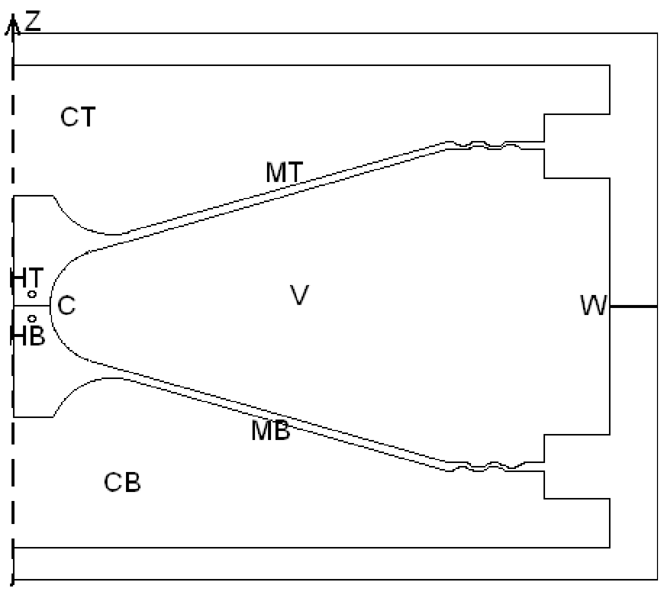

Fig. 1. Geometry of axisymmetric model. CT and CB – top and bottom cavity which are filled with gas, MT and MB – top and bottom membrane, V – vacuum cavity, C – contact surface, W – welded part, HT and HB – points between which temperature difference is measured. HT is heated

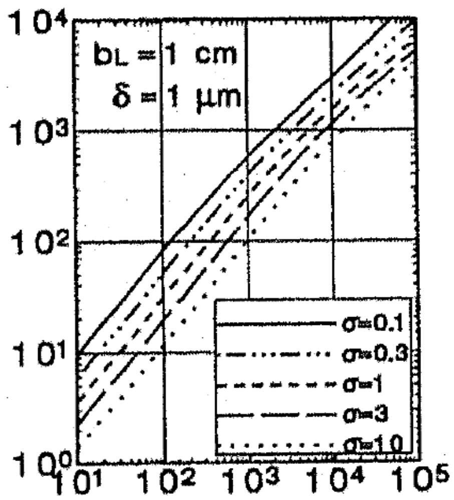

Fig. 2. Contact conductance dependence on contact pressure at different roughness of contact surface. Contact radius – 1 cm. abscissa – apparent contact pressure (kPa), ordinate – thermal contact conductance (W/ m^2 K) [1]

housing and to the other membrane MB can be assured. Polishing both membranes limits radiative heat transfer in the cavity.

Pumping the gas in the cavities CT and CB causes the membranes to deflect and make firm mechanical and thermal contact at surface C. Depending on the magnitude of contact pressure, contact thermal conductance changes and different temperature difference between HT and HB appears – temperature difference decreases if contact pressure increases. Paper [1] contains experimental measurements of contact conductance dependence on pressure at different geometrical properties of contact (diameter, radius of curvature, roughness) – figure 2 shows example of experimental data.

2. Mathematical models

On the outer surface of equipment constant displacement is set – this represents initial deformation determined by welding both parts together. When cavity is filled with gas, the pressure acts on surface of cavity. For mechanical boundary conditions see figure 3.

Material properties used for calculations are shown in table 1. These values corresponds to Ti-6%Al-4%V alloy.

For thermal calculation pressure distribution over contact surface is most important while it is used to set thermal resistance of contact.

On the outer surface of equipment uniform temperature is set. Constant heat generation rate is set in heater element HT (see figure 1).

Two different types of calculations were done. In one-way-coupled simulations

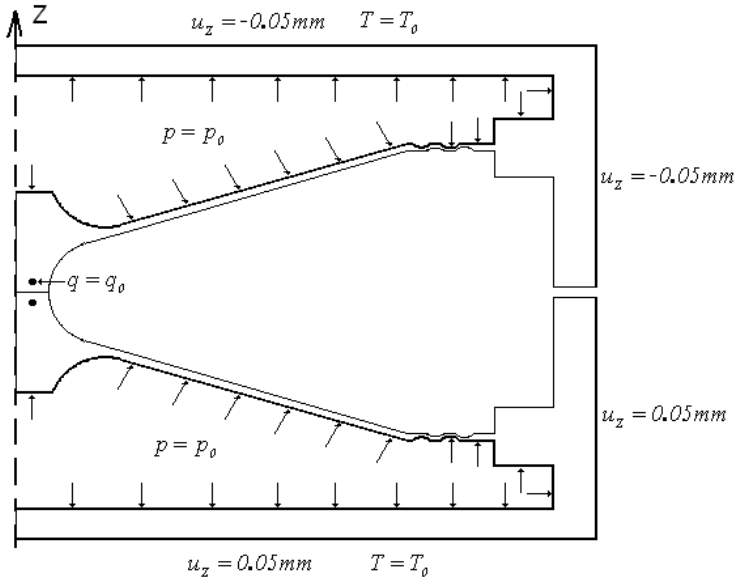

Fig. 3. Boundary conditions

Table 1. Typical physical properties for Ti6Al4V

Properties	**Value**
Density, *kg/m³*	4420
Elastic modulus, *GPa*	114
Poisson's ratio	0.342
Thermal conductivity, *W/m·K*	7.2
Coefficient of thermal expansion, *1/K*	$8.6 \cdot 10^{-6}$

mechanical stress analysis was done first and then obtained contact stresses used for heat and mass transfer. In this case thermal stresses were not considered. In two-way-coupled simulations thermal stresses were included in model, but mass transfer and thermal radiation were neglected. Used methods for solving problem are shown in table 2.

In one-way-coupled simulations contact was modeled as layer – conductivity of layer was adjusted so, that total conductance of layer was the same. It was done due to specific of program – there were no option for contact modelling.

Tab. 2. Different methods used for solving the problem

Model	Coupling	Physical effects neglected
M1 (ANSYS)	Two-way stress ↔ thermal	Heat transfer (conduction, buoyancy and radiation) in gas domains.
M2A (ANSYS)	Two-way stress ↔ thermal	Heat transfer (buoyancy and radiation) in gas domains.
M2B (ANSYS + CFX)	One-way stress → thermal	Thermal stresses, heat transfer (buoyancy and radiation) in gas domains.
M3(ANSYS + CFX)	One-way stress → thermal	Thermal stresses

It is important to establish contact conductance dependence on pressure. Experimental results obtained in [1] were not suitable for this case – smallest contact surface radius in experiment was 1 cm, but in our case it is 0.23 cm. Extrapolation was used to determine the conductance of contact outside 1-10 cm contact radius region. It was figured out that conductance function which fits experiment corresponds to surface roughness between 1 and 3 μm, but this result have to be considered carefully, while we do not know exact shape of conductance function outside 1-10 cm contact radius range. On the other hand these results were useful to determine shape of conduction-pressure function. In experimental data it is obvious that decreasing contact surface radius, conduction increases. Similar shape of dependence function was used:

$$h = B \cdot \hat{p}^{A}. \qquad (1)$$

Here h is thermal conductance, $\hat{p}$ – dimensionless contact pressure, A and B – coefficients which were be found empirically for simulation results to fit experimental results.

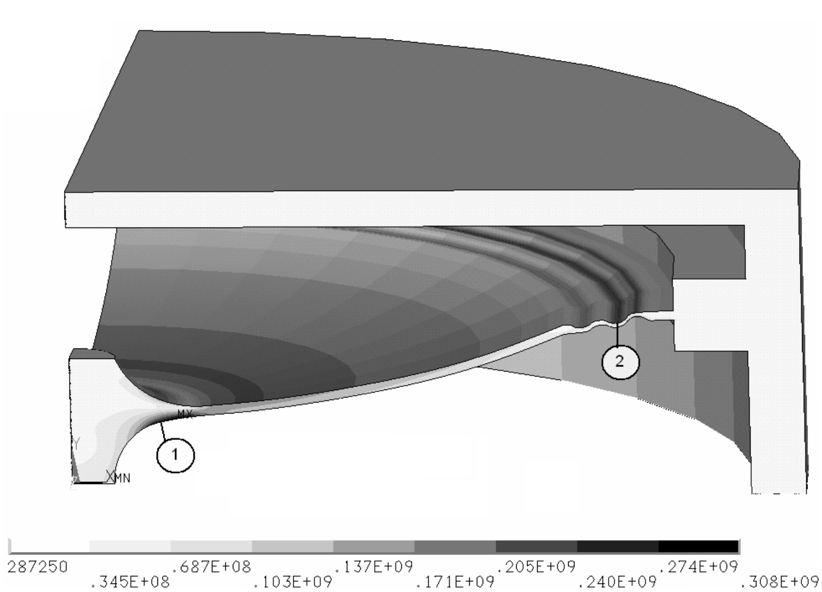

Fig. 4. Von Mises stresses at 5 bar pressure. Only quarter extrusion of top half is shown

3. Numerical simulations

Structural simulations were performed in ANSYS Classic using 2D axisymmetric model. In two-way-coupled stress ↔ thermal simulations both structural and thermal calculations were done in ANSYS. For one way stress → thermal coupling structural calculation was performed in ANSYS and obtained stresses exported to ANSYS CFX for thermal, radiation and hydrodynamic calculations.

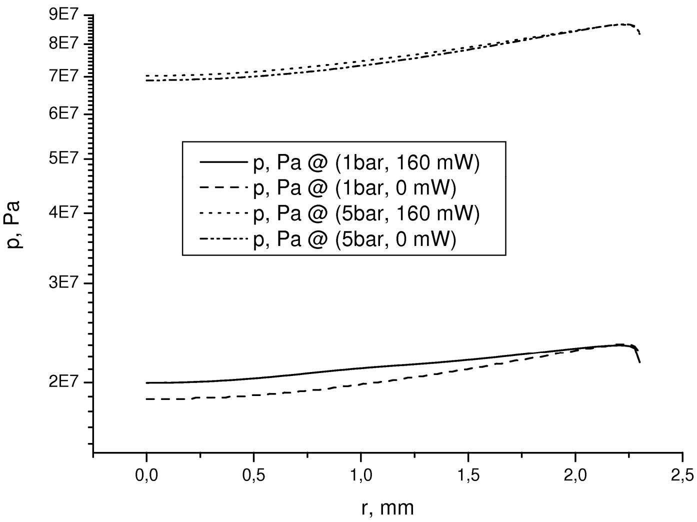

Fig. 5. Thermal stress influence analysis. Stress distribution over radius is shown at 1 and 5 bar pressure with 160 mW heating and no heating (no thermal stresses).

Models M1 and M2A (see table 2) were performed in ANSYS only. Models M2B and M3 – in ANSYS and ANSYS CFX.

Largest model in ANSYS contained approx. 80 thousand of quadratic elements, full CFX simulations – approx. 200 thousand linear elements.

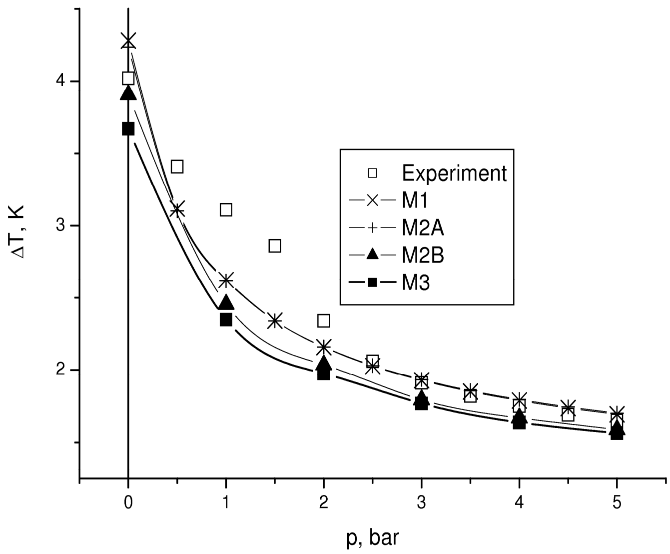

Fig. 6. Temperature dependence on pressure. Comparison of experimental and calculation data. Results obtained using coefficients A=0.85, B= 1.6·mW/(m^2 K) in equation (1).

4. Results

Results show that in modeled pressure range stresses in membrane are lower than maximum allowed for that material (930 MPa). Stress intensity contour plot is shown in figure 4. Large stresses appear in the same regions predicted in previous work [2] (region 2 in figure 4). But maximal stresses appear in region 1, which is due to curve in geometry. Larger radius of curve in this region could decrease maximal stress.

Pressure distribution over contact radius, which is used for determination of contact conductance, is shown in figure 5. Results at 160 mW heating power and no heating power are compared – it is obvious, that thermal stresses cause small change in pressure distribution. Pressure change due to thermal stresses is more important at low gas pressures (up to 7%), while in high pressure region (~ 2%).

Temperature difference dependence on pressure is shown in figure 6. It is obvious that simulation results have different shape than experimental results. It could be due to incorrect shape of conductance function, but three or more parameter function would be very hard to optimize for wide range of physical parameters.

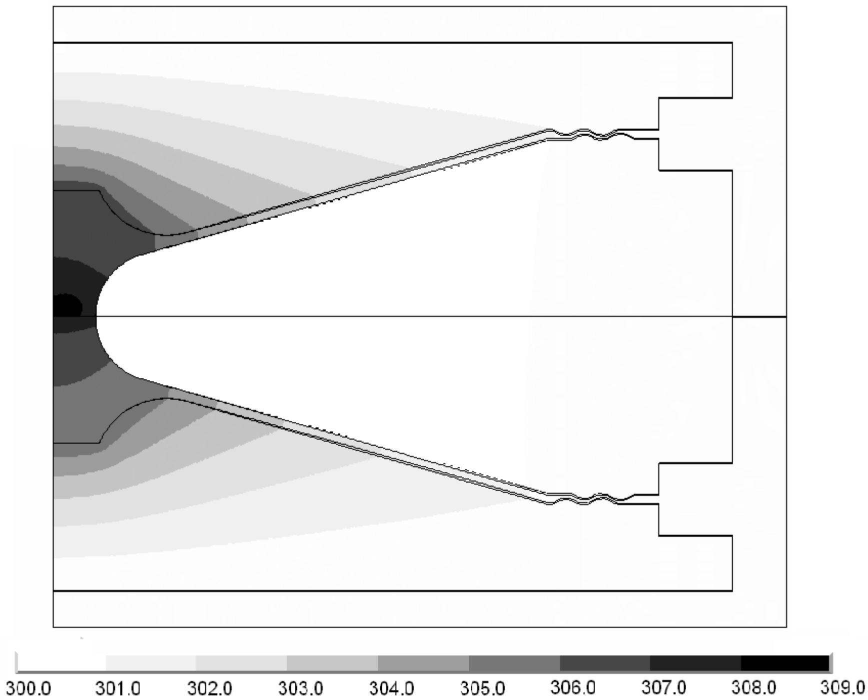

Fig. 7. Temperature field in whole system obtained with model M2A

Local change in slope of experimental curve in 1.0-2.0 bar gas pressure region is not accidental result. It is repeatable experimental effect which is not explained yet. With thermal conduction-pressure dependence function which is used here this effect cannot be described.

In figure 6 it is obvious that the influence of heat transfer in gas is small in the high pressure region where all three models almost fit together, best correspondence is between models, which used same programs (M1 with M2A and M2B with M3). Heat transfer effects in gas are more significant in low pressure region where difference between models is up to 10% (M2B and M3). Comparison of results obtained in different programs (see Table 2) should be considered with precaution. Even when all used parameters are the same (M2A and M2B in figure 6) there are differences between results obtained in ANSYS and CFX. The aspects which can cause differences in results between models in both programs are following:

- Thermal stresses are not coupled with heat analysis in CFX models.
- Contact is modeled as thin layer in CFX.

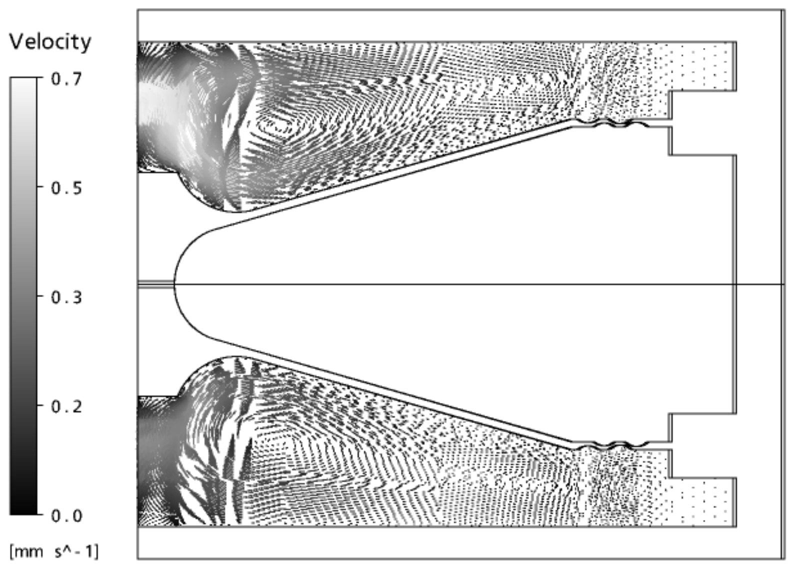

Fig. 8. Velocity field in gas domains

- 2D model in CFX is one element thick sector of cylinder, ANSYS has axial symmetry option.
- CFX uses an element based Finite Volume Method, but ANSYS – Finite Element Method.

Last two aspects are most probable reason, while numerical problems are different in both cases, and the shift in results is probably order of precision. These aspects also cause differences in absolute temperatures in models which use different programs, but temperature differences are still similar. The temperature field obtained with model M2A is shown in figure 7.

The significance of buoyancy is very small because velocity of gas flow is less than 1 mm/s (figure 8). Differences between M2B and M3 (less than 10%) are caused by taking into account buoyancy and thermal radiation. It shows that radiation heat transfer can not be neglected in this parameter region.

Conclusions

Experimental data comparison with numerically obtained results show that used models are calibrated well to describe physical processes in pressure sensor. Structural simulations show that membranes are not overstressed at 5 bar pressure. Stress is about a factor of 30 below the allowed value for this strong material (TiAlV, 930 MPa). Thermal stresses have small influence on the resulting contact pressure – instead of using two-way structural-thermal, one way coupling can be used.

Heat transfer in gas is insignificant in high pressure region and has about 10% influence at low pressures, velocity of gas is small (about 0.7 mm/s). These conclusions allow to use simplified models for further investigation, if needed. Shape of conductance function could be other than used here. More precise determination of conductance-pressure dependence and optimization of geometrical parameters could be a task for further work.

References

[1] M.A. Lambert, S.R. Mirmira, and L.S. Fletcher, Desigh Graphs for Thermal Contact Conductance of Similar and Dissimilar Light Alloys, Journal of Thermophysics and Heat Transfer 20, 2006, pp. 809-816.
[2] V. Frishfelds, A. Jakovics. Estimations of deformation and heat transfer for build up of pressure sensor, Scientific report, Riga, 2007, 14 pp.

Authors

Geza, Vadims;
Prof. Dr. Phys. Jakovics, Andris
Fakulty of Physics and Mathematics
University of Latvia
Zellu str. 8
LV-1002 Riga, Latvia
E-mail: ajakov@latnet.lv

Dr. Phys Thomsen, Knud
Paul Scherrer Institut
CH – 5232 Villigen PSI,
Switzerland
E-mail: knud.thomsen@psi.ch